(unpublished); D. L. Staebler and S. E. Schnatterly, Phys. Rev. B 3, 516 (1971); C. H. Anderson and E. S. Sabisky, *ibid.* 3, 527 (1971); R. C. Alig, *ibid.* 3, 536 (1971).

[6]*Polarons and Excitons*, edited by C. G. Kuper and G. D. Whitfield (Plenum, New York, 1963).

[7]J. Appel, in *Solid State Physics*, edited by F. Seitz, D. Turnbull, and H. Ehrenreich (Academic, New York, 1968), Vol. 21.

[8]H. S. Bennett, Phys. Rev. 169, 729 (1968).

[9]J. Dresner, Phys. Rev. 143, 558 (1966); J. Chem. Phys. 52, 6343 (1970).

[10]W. J. Scouler and A. Smakula, Phys. Rev. 120, 1154 (1960).

[11]D. Howarth and E. Sondheimer, Proc. Roy. Soc. (London) A219, 53 (1953).

[12]R. L. Petritz and W. W. Scanlon, Phys. Rev. 97, 1620 (1955).

[13]F. Garcia-Moliner, Phys. Rev. 130, 2290 (1963).

[14]J. W. Hodby, J. A. Borders, F. C. Brown, and S. Foner, Phys. Rev. Letters 19, 952 (1967).

PHYSICAL REVIEW B VOLUME 3, NUMBER 8 15 APRIL 1971

X-Ray Photoelectron Spectroscopy of Solids; Evidence of Band Structure

T. Novakov

Shell Development Company, Emeryville, California 94608

(Received 2 November 1970)

X-ray photoelectron spectra of solid Cu_2O, CuCl, CuO, CuS, and $CuSO_4$ were measured. In all cases, satellites having various degrees of complexity are seen adjacent to the (Cu) $2p$ photolines. A multiple-excitation mechanism is proposed for the explanation of these satellites. The satellites are formed when the emission of a $2p$ photoelectron takes place in parallel with a valence-band–conduction-band excitation. These photolines are thus emitted with kinetic energies lowered by the amounts of allowed interband transitions.

I. INTRODUCTION

X-ray photoelectron spectroscopy is successfully being applied to elucidate problems of molecular structure by measuring the electron core-level binding energies.[1] Both solids and gases are studied. Binding energies are known to depend on the charge of the atom in the molecule.[1,2] Valence-electron structure has also been investigated, mostly in the case of free gaseous molecules. The same technique has been extensively used to study Auger-electron emission from both atoms and molecules.[3] Most of the work done in this field, however, relates to chemical problems.

In this paper, some photoelectron experiments will be described, which seem to have a direct relation to electronic properties of solids. The method of photoelectron spectroscopy is basically very simple. The solid whose photoelectron spectrum is to be investigated is irradiated by a "monochromatic" x ray, for example, by Mg $K\alpha$($h\nu$ = 1253.6 eV) or Al $K\alpha$($h\nu$ = 1486.6 eV) radiation. These radiations have an intrinsic width of about 1 eV, which sets the limit on the linewidth. The emitted photoelectrons are analyzed by a high-resolution electron spectrometer.

From the conservation of energy it follows that

$$h\nu = E^f - E^i + E_{\rm kin} + \phi \ ,$$

where E^f and E^i are the total final and initial energies of the system. $E_{\rm kin}$ is the kinetic energy of the ejected electron and ϕ is the contact potential difference between the sample surface and the spectrometer. If there are several final states possible then there will be, at least in principle, a corresponding number of photoelectron lines emitted from a given subshell.

For a simple one-electron process, E^f would correspond to a vacancy in the level, and the difference $E^f - E^i$ would be equal to the electron binding energy of that level. In this case, a single photoline is seen. In other cases, complex lines may appear in the spectrum. In this investigation, we were looking particularly for cases of line splittings and line satellites. Less attention has been paid to the absolute energies of photolines and therefore all our quoted binding energies are nominal.

II. EXPERIMENTAL TECHNIQUE

The experiments described in this work have been performed with the Varian IEE-15 electrostatic spectrometer, utilizing Al $K\alpha$ radiation. The analyzer part of the spectrometer was set to transmit electrons of a preset energy. Typically, this energy may be between 30 and 100 eV. The scanning of the spectrum is done by stepping a positive bias voltage applied to the sample. Provision, however, was made that the immediate vicinity of the sample was in a field-free region, although at a positive potential with respect to the rest of the spectrometer. The advantage of this mode of operation is that the spectrometer contribution to the

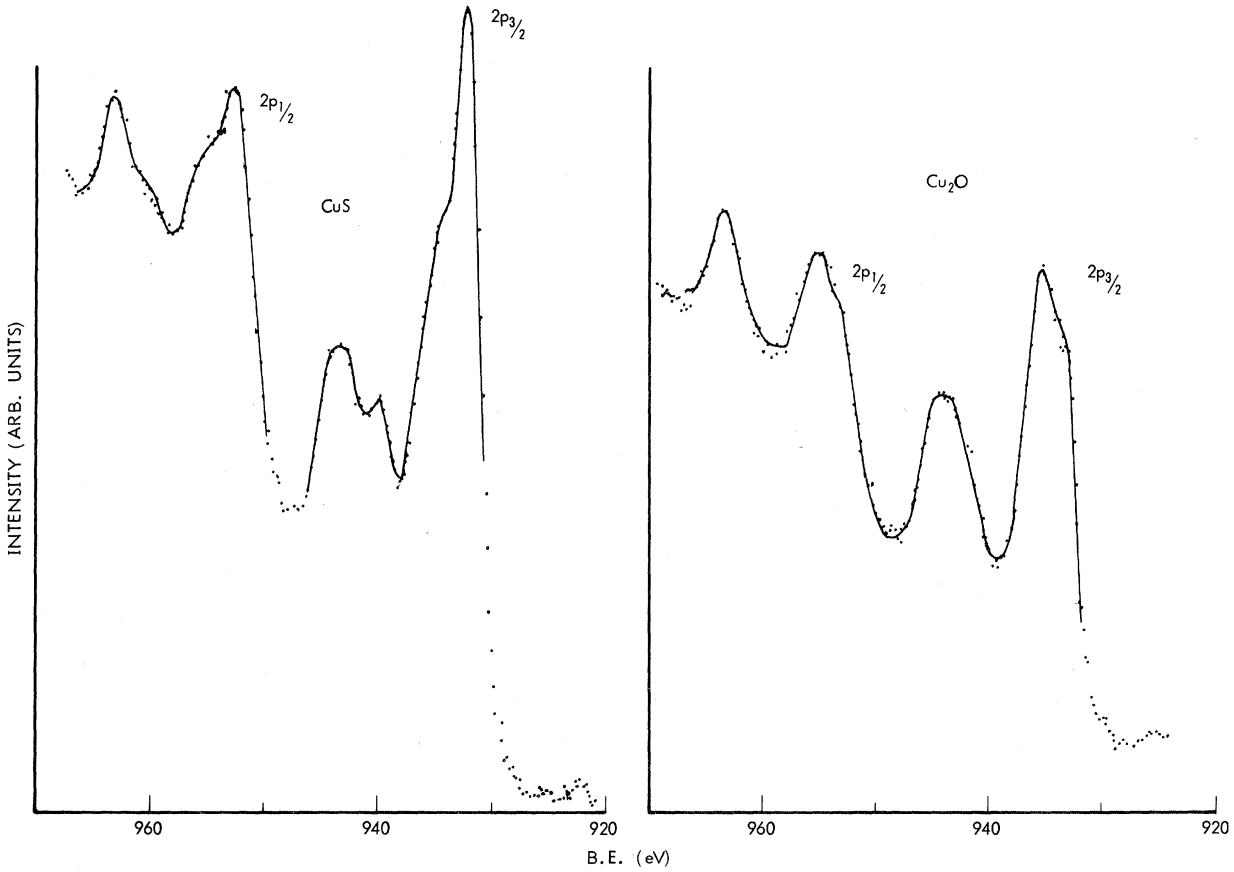

FIG. 1. $2p_{1/2}$ and $2p_{3/2}$ photolines and their satellites for CuS and Cu2O excited by Al $K\alpha$. Note the difference in the satellite structure between the two compounds. Satellites are absent in the $3s$-$3p$ region (Fig. 2).

linewidth is constant throughout the entire spectrum.

Samples were in all cases solid powders deposited on Scotch tape. A virtual electron source is formed in front of the sample by means of a narrow slit. In this way, there is no significant difference in the instrumental linewidth caused by slight variation of the sample length and width among different samples.

Spectral regions covering lines of interest were scanned one after the other and, as a rule, when long repetitive scans were needed to measure weak lines, a pair of strong lines was measured at the beginning and at the end of each run. This was found to be a good measure of the spectrometer stability and also of the chemical stability of the sample. Only those cases were considered where no shifts in the line positions were noticed. Each compound was measured at least two times with freshly prepared samples.

III. RESULTS AND DISCUSSION

We have investigated a number of copper compounds such as the cuprous Cu_2O, CuCl with Cu free-ion configuration $3p^6 3d^{10}$, and cupric CuO, CuS, and $CuSO_4$ with configuration $3p^6 3d^9$. The photoelectron spectra of these mostly semiconducting compounds are quite strange, with complex satellite structures associated with (Cu) $2p_{1/2}$ and $2p_{3/2}$ photolines. The $3s$ and $3p$ regions were free of these pronounced satellites.

Figure 1 illustrates this point. Here we see the (Cu) $2p_{1/2}$ and $2p_{2/3}$ lines for CuS and Cu_2O. To the left of the main $2p$ lines (i.e., at lower kinetic energies), a satellite structure is seen which is distinctly different for the two compounds. The $3s$ and $3p$ lines are obviously not associated with satellites to the same extent as the $2p$ lines, as is seen from Fig. 2.

The bars drawn at the half-maxima of the $3s$ and $3p$ lines represent the widths of metallic copper lines. It is evident that the two $3s$ lines are different in width and in shape. The one corresponding to the cuprous oxide is single and narrow in comparison with the $3s$ line of cupric sulfide, which shows a splitting of about 4 eV. Such a behavior can be expected when there are unpaired d electrons in the valence band.[4-6]

Let us now return to the $2p$ satellites. Several

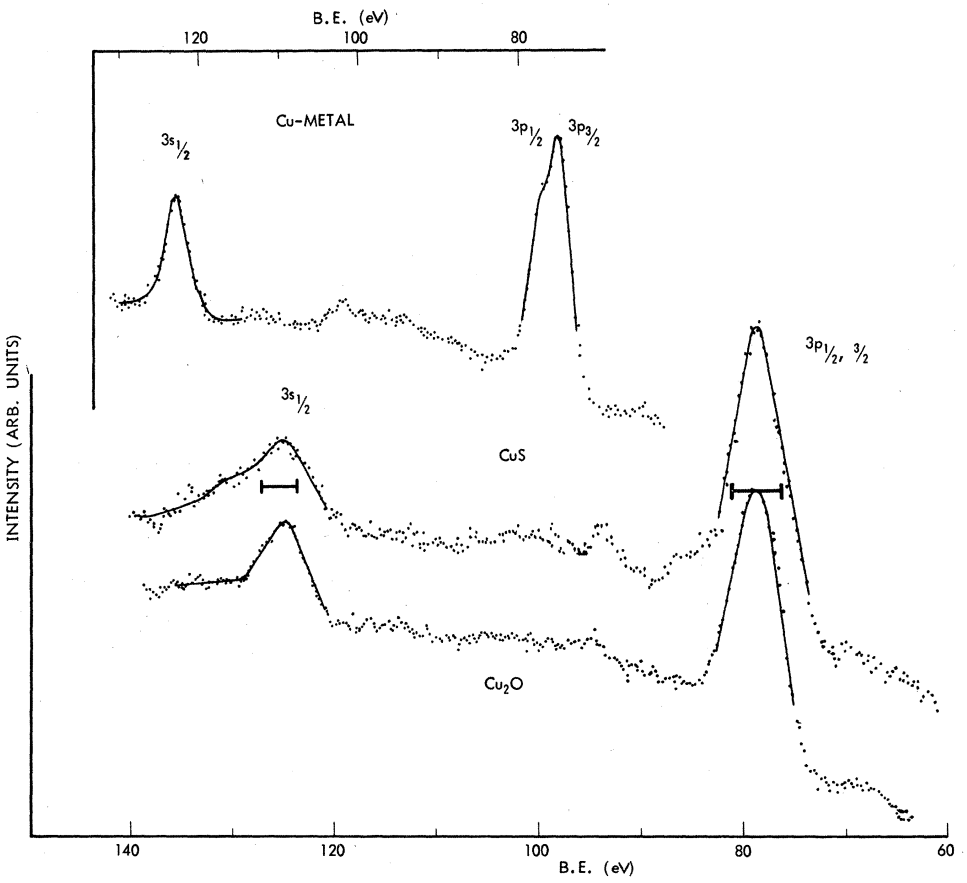

FIG. 2. (Cu) 3*s* and 3*p* photolines from metallic Cu, CuS, and Cu_2O excited with Al $K\alpha$ radiation. 3*s* line of cupric sulfide shows a splitting of about 4 eV indicative of the presence of unpaired *d* electron. Cuprous oxide having filled 3*d* shell shows no splitting. Bars drawn at the half-maxima indicate the corresponding linewidths in Cu metal. Binding energies (nominal) are given in electron volts.

alternative explanations for their existence can be postulated. For example, the satellites might be essentially 2*p* photoelectron lines from different kinds of copper ions. These ions would have to be highly positively charged to account for the large chemical shift of up to 10 eV. This explanation fails because no similar structure is associated with the 3*s* and 3*p* lines. The chemical shifts are similar for all levels accessible by Al or Mg $K\alpha$ radiation. Moreover, the chemical shift between copper compounds with formal oxidation states of +2 and +1 is only about 1.5 eV. The conclusion is therefore that the satellites are not the result of a chemical shift between different species of Cu.

The second possibility is that the satellites are Auger electrons. This possibility can also be dismissed. If these extra peaks were Auger lines they would not be seen next to the Cu 2*p* lines if Mg $K\alpha$ radiation were used instead of Al $K\alpha$. We have performed such an experiment and therefore rule out this alternative.

The third possibility might be that the satellites are caused by the discrete energy losses suffered by electrons in inelastic collisions. Those losses are however expected to be practically the same for the two close lying 2*p* photoelectron lines. Furthermore they should be also associated to some extent with other photoelectron lines in the spectrum such as (O) 1*s*, (S) 2*s*, 2*p*, (Cu) 3*p*, etc.

The fourth possibility could be, and evidence will be presented that this is indeed the case, a process involving excitations of electrons from the valence band to unoccupied states in the conduction band, taking place in parallel with the formation of a 2*p* vacancy. The emitted photoelectrons will then have kinetic energies reduced by the amounts corresponding to these interband transitions. The satellite spectrum would thus reveal the band structure of the solid.

The observed spectrum is thus a reflection of the density of states in both the valence and the unoccupied conduction band, weighted by the transition probabilities.

Different compounds should in principle show different structure. That this is the case is evident from Fig. 1. Other examples are shown in Fig. 3, where the $2p_{1/2}$ and $2p_{3/2}$ regions from metallic copper, $CuSO_4$ and CuO are shown. The CuO was also measured with higher resolution to study the doublet structure of one of the satellites. The origin of this doublet, and also of some other satellite doublets, may be related to a multiplet-type splitting or to the possibility that the transition probabilities may be different when the primary excitation is in

the $2p_{3/2}$ level. In that case, the doublet should also be present in the $2p_{1/2}$ satellite, but appearing with a different intensity ratio.

Effects similar to the one just described are known to exist in the case of free atoms. In the atomic case, this type of multiple excitation is explained by the so-called shakeoff theory[7] (sudden approximation), according to which both excited and ionized atoms may appear in the final state. This effect has been verified experimentally by using both electrons and photons to produce primary vacancies.[8]

Satellites accompanying KLL Auger electrons emitted from solid KCl and K_2SO_4 have been observed by Fahlman *et al.*[9] They suggested that these satellites are emitted in a nonradiative process where the electron configuration of the final state has two vacancies in the $2p$ shell and one peripheral electron promoted to an excited state. In addition, there could also be a removal of peripheral electrons into the continuum, leaving the potassium ion in a state of multiple ionization.

As far as the copper compounds are concerned it would be of interest to compare the energies of the satellites, with respect to the original $2p$ lines, with measured optical transitions taking place between the valence band and the conduction band. Such measurements exist for cuprous halides such as CuCl, CuBr, and CuI.[10] We have measured the photoelectron spectrum of CuCl and the result is shown in Fig. 4. Satellites with visible structure are seen. The optical measurements give the following transitions for CuCl: 3.306 ($\Gamma_{15} \rightarrow \Gamma_1$), 6.1 ($\Gamma_{15} \rightarrow \Gamma_{15}$), 6.4 ($\Lambda_3 \rightarrow \Lambda_1$), 8.3 ($X_5 \rightarrow X_1$), 10.0 ($X_5 \rightarrow X_3$), with energies in electron volts. These are indicated in the CuCl photoelectron spectrum in Fig. 4. As one can see, there is a correspondence. The optical transitions are of dipole nature, while the "shakeup" excitation is monopole in character, at least in the atomic case. In solids it may be possible to have allowed transitions of similar energy taking place in the vicinity of optical transi-

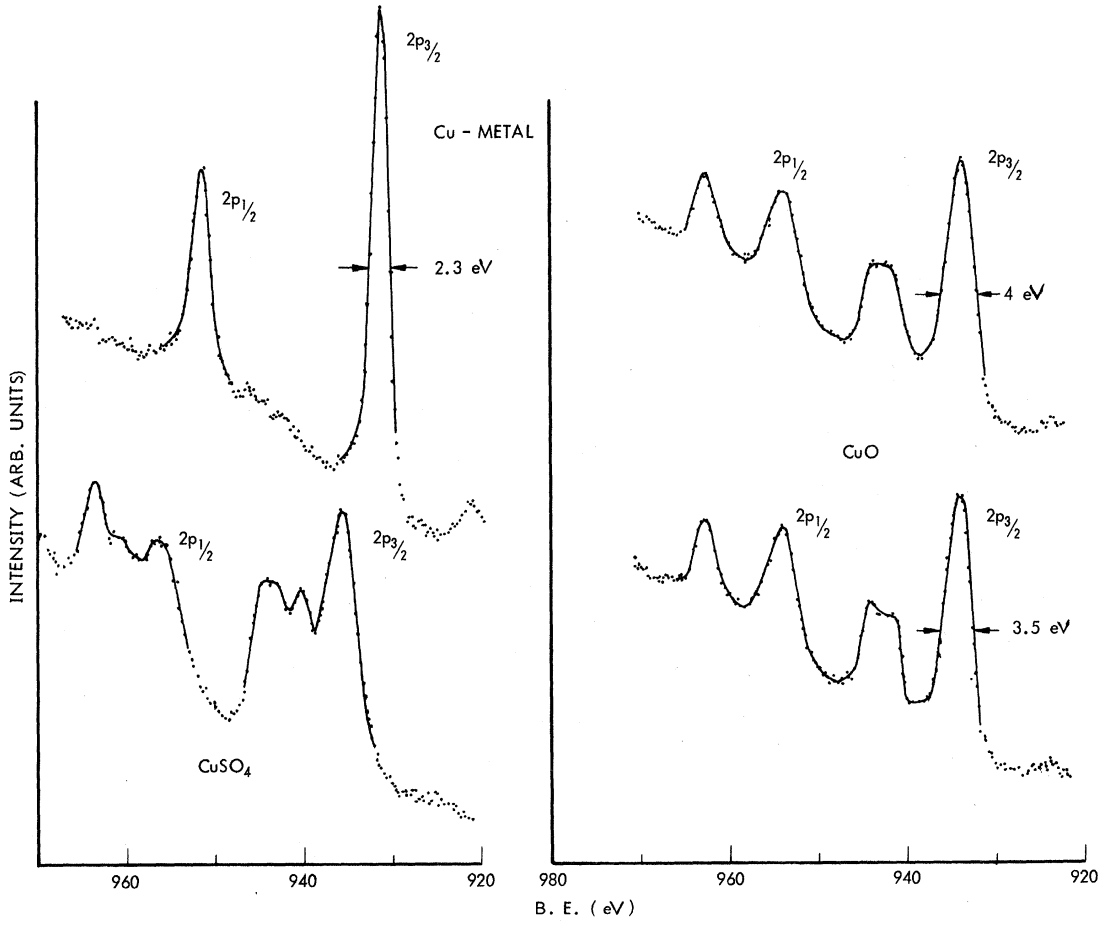

FIG. 3. $2p_{1/2}$ and $2p_{3/2}$ region of metallic Cu, $CuSO_4$, and CuO. Satellites are seen in the two compounds but not in Cu metal. CuO spectrum measured with improved resolution is also seen. Note the difference in $2p$ linewidth between metallic Cu (2.3 eV) and CuO (4.0 eV).

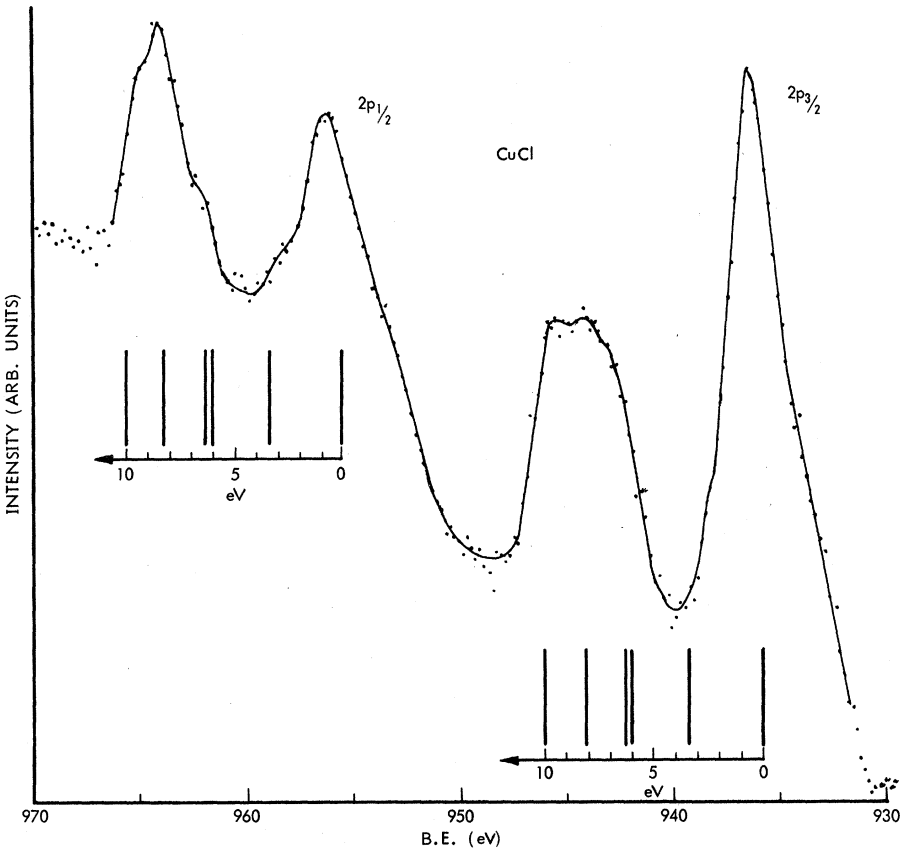

FIG. 4. $2p_{1/2}$ and $2p_{3/2}$ photolines and their satellites in CuCl. The valence-band–conduction-band transition energies, as obtained from optical measurements (Ref. 10) are shown in the figure. Correspondence is seen between these energies and the satellite structure. Note the different relative intensities in the two groups of satellites.

tions. The lack of ideal agreement is not unexpected considering the difference in the nature of these two processes. Here we are comparing transitions in a neutral configuration with the transitions in a system with an inner-shell vacancy. The presence of this vacancy may cause changes in the band structure and lead to changes in the excitation energy in some cases. The problem is somewhat similar in x-ray absorption spectroscopy. Our main conclusion is however, that the energy interval deduced from photoelectron-line satellites is nearly the same as the one obtained from the optical work.

It is interesting to note that the transition probabilities may actually be different, depending on where the primary vacancy occurs. Note the different relative intensities, corresponding to different transitions, in the $2p_{1/2}$ and $2p_{3/2}$ satellites.

ACKNOWLEDGMENTS

The author has profited from discussions with Dr. J. W. Otvos, Dr. C. D. Wagner, Dr. T. L. Barr, Dr. T. A. Carlson, and Dr. P. S. Bagus. R. C. Schmidt is acknowledged for his help with the experiments.

[1]K. Siegbahn, C. Nordling, A. Fahlman, R. Nordberg, K. Hamrin, J. Hedman, C. Johansson, T. Bergmark, S. E. Karlsson, I. Lindgren, and B. Lindberg, *ESCA-Atomic, Molecular, and Solid State Structure Studied by Means of Electron Spectroscopy* (Almqvist and Wiksells, Uppsala, 1967).

[2]J. M. Hollander, D. N. Hendrickson, and W. L. Jolly, J. Chem. Phys. 49, 3315 (1968); D. N. Hendrickson, J. M. Hollander, and W. L. Jolly, J. Am. Chem. Soc. 8, 2642 (1969).

[3]See, for example, K. Siegbahn, C. Nordling, C. Johansson, J. Hedman, P. F. Heden, K. Hamrin, U. Gelius, T. Bergmark, L. O. Werme, R. Manne, and Y. Baer, *ESCA Applied to Free Molecules* (North-Holland, Amsterdam, 1969).

[4]R. E. Watson and A. J. Freeman, in *Hyperfine Interactions*, edited by A. J. Freeman, (Academic, New York, 1967).

[5]J. Hedman, P. F. Heden, C. Nordling, and K. Siegbahn, Phys. Letters 29A, 178 (1969).

[6]C. S. Fadley, D. A. Shirley, A. J. Freeman, P. S. Bagus, and J. V. Mallow, Phys. Rev. Letters 23, 1397 (1969).

[7]M. O. Krause, T. A. Carlson, and R. D. Dismukes, Phys. Rev. 170, 37 (1968); T. Åberg, *ibid.* 156, 35 (1967).

[8]G. Graeffe, J. Siivola, J. Utriainen, M. Linkoaha, and T. Åberg, Phys. Letters 29A, 464 (1969); also M. O. Krause, I. A. Stevie, L. U. Lewis, T. A. Carlson, and W. E. Moddeman, *ibid.* 31A, 81 (1970).

[9]A. Fahlman, K. Hamrin, G. Axelson, C. Nordling, and K. Siegbahn, Z. Physik 192, 484 (1966).

[10]J. Tauc, in *Progress in Semiconductors* (Temple, London, 1965), Vol. 9, p. 120.

PHYSICAL REVIEW B VOLUME 3, NUMBER 8 15 APRIL 1971

Frequency Upconversion in $YF_3 : Yb^{3+},Tm^{3+}$

F. W. Ostermayer, Jr., J. P. van der Ziel, H. M. Marcos, L. G. Van Uitert, and J. E. Geusic

Bell Telephone Laboratories, Murray Hill, New Jersey 07974

(Received 5 October 1970)

The stepwise conversion of infrared ($\approx 0.97\ \mu$) radiation to near infrared ($0.81\ \mu$) and visible ($0.475\ \mu$) light in YF_3 sensitized with Yb^{3+} and activated with Tm^{3+} has been studied in detail. The lifetimes and fluorescence intensities of the important manifolds (Yb $^2F_{5/2}$, Tm $^3H_4$, Tm $^3F_4$, and Tm $^1G_4$), as well as the Yb-to-Tm transfer probability coefficients for the three steps of the process, have been measured as functions of concentration. A saturation effect previously observed in the Tm emission versus infrared excitation intensity has been shown to result from the rate of depopulation of Tm $^3H_4$ by the second Yb-to-Tm transfer exceeding the Tm $^3H_4$ decay rate. This was used to determine the second transfer probability coefficient. The first transfer probability coefficient was found to be 1.2×10^{-17} cm^3sec^{-1} independent of Tm concentration and for Yb concentration of the order of 10 at.% and greater. The second transfer probability coefficient was found to be approximately 10^{-14} cm^3sec^{-1} for Yb concentrations of 25 at.% and greater. The third transfer probability coefficient was found to be 2.7×10^{-16} cm^3sec^{-1}. The dependence on Yb concentration of the relative efficiency of conversion to 0.475-μ light agrees well with the values calculated from a rate-equation model using the measured lifetimes and transfer probability coefficients.

I. INTRODUCTION

The conversion of infrared ($\approx 0.97\ \mu$) radiation to near infrared ($0.81\ \mu$) and visible ($0.475\ \mu$) light has been observed[1-5] in a number of host crystals sensitized with Yb^{3+} and activated with Tm^{3+}. Since the conversion process is particularly efficient in YF_3,[5] a detailed study has been made to correlate the efficiency with the characteristics of Yb and Tm in this material. This paper presents the results of the study.

Section II discusses the model for the conversion process and pertinent results are derived from the rate equations. The assumptions implicit in the rate equations are also discussed. Section III deals with the fluorescence lifetime and intensity measurements of the important Yb and Tm levels and Sec. IV with the Yb-to-Tm transfer probabilities. In Sec. V, these results are used to calculate the conversion efficiency. Reasonable agreement with the experimental efficiency and with the variation of efficiency with Yb concentration is obtained.

II. CONVERSION MECHANISM AND RATE EQUATIONS

The model for the conversion process which agrees with our observed results is that proposed by Auzel[1] involving stepwise excitation of Tm by nonresonant energy transfer from Yb and multiphonon decay in Tm. The mechanism is illustrated schematically on the Yb and Tm energy-level diagrams[6] in Fig. 1. To the right-hand side of each manifold is its spectroscopic label, and to the left-hand side is a label which is more conveniently used in the rate equations below. Step 1 is a nonresonant transfer in which 1650 cm^{-1} must be absorbed by the lattice, 1′ is a multiphonon decay, 2 is a nonresonant transfer with 1000 cm^{-1} absorbed by the lattice, 2′ are multiphonon decays, and 3 is a nonresonant transfer with 1400 cm^{-1} absorbed by the lattice. The 0.81-μ emission results from the Tm $^3F_4 \rightarrow {}^3H_6$ transition and that at $0.475\ \mu$ from Tm $^1G_4 \rightarrow {}^3H_6$.

The steady-state rate equations appropriate to this model are

$$\frac{dn_{Y2}}{dt} = \frac{\sigma_Y I}{\epsilon_Y} n_{Y1} - \frac{n_{Y2}}{\tau_Y} - \chi_1 n_{Y2} n_{T1} - \chi_2 n_{Y2} n_{T2} - \chi_3 n_{Y2} n_{T4} = 0 , \quad (1)$$

$$\frac{dn_{T2}}{dt} = \chi_1 n_{Y2} n_{T1} - \frac{n_{T2}}{\tau_{T2}} - \chi_2 n_{Y2} n_{T2} = 0 , \quad (2)$$

$$\frac{dn_{T4}}{dt} = \chi_2 n_{Y2} n_{T2} - \frac{n_{T4}}{\tau_{T4}} - \chi_3 n_{Y2} n_{T4} = 0 , \quad (3)$$

$$\frac{dn_{T7}}{dt} = \chi_3 n_{Y2} n_{T4} - \frac{n_{T7}}{\tau_{T7}} = 0 , \quad (4)$$

where σ_Y is the Yb $^2F_{7/2} \rightarrow {}^2F_{5/2}$ cross section averaged over the spectrum of the exciting radiation, ϵ_Y is the average energy of the Yb $^2F_{7/2} \rightarrow {}^2F_{5/2}$ transition, I is the total intensity of the exciting